University of Plymouth

PEARL **https://pearl.plymouth.ac.uk**

01 University of Plymouth Research Outputs University of Plymouth Research Outputs

2005-10-01

Up-regulation of delta-like 4 ligand in human tumor vasculature and the role of basal expression in endothelial cell function.

Patel, NS

http://hdl.handle.net/10026.1/10306

10.1158/0008-5472.CAN-05-1208
Cancer Res

All content in PEARL is protected by copyright law. Author manuscripts are made available in accordance with publisher policies. Please cite only the published version using the details provided on the item record or document. In the absence of an open licence (e.g. Creative Commons), permissions for further reuse of content should be sought from the publisher or author.

Up-regulation of Delta-like 4 Ligand in Human Tumor Vasculature and the Role of Basal Expression in Endothelial Cell Function

Nilay S. Patel,[1,2] Ji-Liang Li,[1] Daniele Generali,[1] Richard Poulsom,[3] David W. Cranston,[2] and Adrian L. Harris[1]

[1]Molecular Oncology Laboratories, Cancer Research UK, Weatherall Institute of Molecular Medicine, John Radcliffe Hospital; [2]Department of Urology, Churchill Hospital, University of Oxford, Oxford; and [3]In Situ Hybridization Service, Cancer Research UK, London, United Kingdom

Abstract

The Notch signaling pathway and the delta-like 4 ligand (DLL4) play key roles in embryonic vascular development. Many of the pathways involved in embryonic vascular development also play important roles in tumor angiogenesis. In this study, we assessed the expression of DLL4 in primary renal cancer and investigated the biological function of DLL4 in primary endothelial cells. Using real-time quantitative PCR and *in situ* hybridization, we showed that the expression of DLL4 was up-regulated within the vasculature of clear cell-renal cell carcinoma almost 9-fold more than normal kidney and was correlated with the expression of vascular endothelial growth factor (VEGF). The expression of DLL4 in endothelial cells was up-regulated by VEGF and basic fibroblast growth factor synergistically, and by hypoxia through hypoxia-inducible factor 1α. Down-regulation of DLL4 expression with RNA interference led to decreased expression of HEY1 and EphrinB2, and the inhibition of endothelial cell proliferation, migration, and network formation, all of which are important processes in tumor angiogenesis. The inhibition of proliferation occurred via the induction of cell cycle arrest in G_0-G_1 by increased expression of p21 and decreased phosphorylation of retinoblastoma. We conclude that an optimal window of the DLL4 expression is essential for tumor angiogenesis and that selective modulation of the DLL4 expression within human tumors may represent a potential novel antiangiogenic therapy. (Cancer Res 2005; 65(19): 8690-7)

Introduction

Tumor angiogenesis is an important process in tumor growth and metastatic progression (1). Many solid tumors are known to develop hypoxic microenvironments as a result of insufficient or aberrant blood supplies. Activation of the hypoxia-inducible factors HIF-1α and HIF-2α in response to hypoxia leads to the up-regulation of numerous adaptive proteins, including angiogenic factors such as vascular endothelial growth factor (VEGF; ref. 2).

Many of the processes involved in tumor angiogenesis are mirrored during embryonic vascular development. In the past decade, the Notch signaling pathway has been shown to play a key role in vascular development. The Notch pathway is an evolutionary conserved intercellular signaling pathway involved in numerous biological processes including cell fate determination, cellular differentiation, proliferation, survival, and apoptosis (3–5). In mammalian cells, there are five transmembrane Notch ligands [Jagged1, Jagged2, delta-like 1 ligand (DLL1), DLL3, and DLL4] and four Notch receptors (Notch1-4). Ligand-receptor binding activates the signaling pathway by initiating the cleavage of the Notch intracellular domain from the cell membrane (6, 7). The Notch intracellular domain subsequently translocates to the nucleus where it classically interacts with the transcription factor C promoter binding factor 1 (CBF1)/recombination signal binding protein Jκ (RBP-Jκ)/Suppressor of Hairless [Su(H)]/Lag-1 protein (CSL). The basic helix-loop-helix-orange proteins (bHLH) Hairy/Enhancer of Split (HES1, 5, and 7) and the HES-related proteins (HEY1, HEY2, and HEYL) are the best-characterized downstream targets of the Notch intracellular domain/CSL complex (8–10).

Mice deficient for various Notch components die *in utero* of severe vascular abnormalities (11). DLL4 knockout mice display vascular defects similar in pattern to those seen in Notch1/Notch4 double knockouts. Interestingly, haploinsufficiency of DLL4 also results in embryonic lethality from severe vascular defects (12–14). Haploinsufficiency for angiogenic factors is uncommon and highlights the importance of DLL4 over and above other components of the Notch pathway. Similar phenotypes have been only described for VEGF knockout mice (15, 16).

We and others have previously shown that DLL4 is expressed at sites of vascular development and angiogenesis (14, 17, 18). During early embryonic development, DLL4 is initially observed in major arterial vessels; with embryonic maturation, this pattern of expression disappears whereupon it is confined to small vessels and capillaries. DLL4 is up-regulated at sites of physiologic and pathologic angiogenesis (17). It is high in ovarian vessels surrounding growing follicles and is up-regulated within the tumor vasculature when compared with adjacent normal tissues. Xenograft studies showed high expression of mouse DLL4, but not of human-derived DLL4, within the tumor vasculature. We have shown *in vitro* that DLL4 is a hypoxia-regulated gene, although the pathway was unknown (17).

In this study, we investigated the expression of DLL4 in renal tumors, analyzed the relationship between DLL4, hypoxia, and angiogenic growth factors, and assessed the biological function of DLL4 in tumor angiogenesis.

Materials and Methods

Cells and tissue samples. Human umbilical vein endothelial cells (HUVEC) were isolated from fresh human umbilical cords by infusion with 0.1% collagenase (Sigma-Aldrich, St. Louis, MO). Human aortic endothelial

Requests for reprints: Ji-Liang Li, Cancer Research UK, Weatherall Institute of Molecular Medicine, John Radcliffe Hospital, Oxford OX3 9DS, United Kingdom. Phone: 44-1865-222457; Fax: 44-1865-222431; E-mail: lij@cancer.org.uk or aharris.lab@cancer.org.uk.

©2005 American Association for Cancer Research.

doi:10.1158/0008-5472.CAN-05-1208

Downloaded from cancerres.aacrjournals.org on May 9, 2015. © 2005 American Association for Cancer Research.

cells (HAEC) were obtained from PromoCell (Heidelberg, Germany). Human iliac artery endothelial cells (HIAEC) and human femoral artery endothelial cells (HFAEC) were purchased from LGC Promochem (London, United Kingdom). Endo742, a gift from Mike O'Hare (University College London, London, United Kingdom), is an immortalized normal human breast endothelial cell line (19). All tissue cultures were done using MCDB131 medium containing HEPES (4.8 g/L), 20% heat inactivated FCS, 50 μg/mL endothelial cell growth supplement (ECGS), 5 IU/mL heparin, 100 IU/mL penicillin, 100 μg/mL streptomycin, and 2 mmol/L glutamine (Sigma-Aldrich). Cells were incubated at 37°C in a humidified atmosphere of 5% CO_2. Cells exposed to hypoxia were incubated for 16 hours at 0.1% O_2 and 5% CO_2. Cells were not used beyond passage 6. Human tissue samples were obtained postoperatively from the Department of Urology, Churchill Hospital (Oxford, United Kingdom). All patients gave signed, informed consent for their tissues to be used for scientific research. Areas of normal tissue and tumor were identified by Dr. D.R. Davies (Consultant Pathologist, John Radcliffe Hospital, Oxford, United Kingdom).

RNA interference. Chemically synthesized gene-specific small interfering RNA (siRNA) duplexes were designed, BLAST searched, and manufactured by Eurogentec (Seraing, Belgium) as per accepted guidelines (20). The following siRNA sequences were used: DLL4-Duplex1 (20 nmol/L): CUACUAUGGAGA-CAACUGCTT; DLL4-Duplex2 (20 nmol/L): UGACCACUUCGGCCACUAUTT; DLL4 scrambled control (20 nmol/L): UCUGAAAAGCACGCUUGACTT; HIF-1α (50 nmol/L): CUGAUGACCAGCAACUUGATT; HIF-2α (50 nmol/L): CAGCAUCUUUGAUAGCAGUTT; and HIF scrambled control (50 nmol/L): AGUUCAACGACCAGUAGUCTT. Transfection of siRNA duplexes was done with cells at 40% to 50% confluency using 3 mL of Optimem-1 and 12 μL of Lipofectamine 2000 (Invitrogen, Carlsbad, CA). Biological functional assays and gene expression analysis were done 24 hours after siRNA transfection.

RNA extraction and reverse transcription. Extraction of total RNA from cultured endothelial cells was done using TRI-Reagent (Sigma-Aldrich) as per instructions of the manufacturer. The quality of RNA extracted was assessed using RNA 6000 Nano Chips and the Agilent 2100 Bioanalyzer (Agilent Technologies, Palo Alto, CA). cDNA was synthesized by reverse transcribing total RNA with the High Capacity cDNA Archive Kit (Applied Biosystems, Foster City, CA).

Real-time quantitative PCR. Real-time quantitative PCR reactions were done in triplicate using the Corbett Research Rotor Gene RG-3000 (Sydney, Australia). Each reaction was done in an individual tube and made to 25 μL containing the equivalent of 5 ng reverse-transcribed RNA (1 ng in the case of 18S rRNA), 12.5 μL TaqMan 2× PCR Master Mix (Applied Biosystems), and 1.25 μL the probe/primer mix. Human β-actin (renal samples) and eukaryotic 18S rRNA (endothelial cells) were used as reference genes to normalize for differences in the amount of total RNA in each sample. The following primer/probe kits were purchased as Assays-on-Demand from Applied Biosystems: DLL4 (Hs00184092_m1), HES1 (Hs00172878_m1), HEY1 (Hs00172878_m1), HEY2 (Hs00232622_m1), Ephrin B2 (Hs00187950_m1), VEGFR2 (Hs00176676_m1), CD34 (Hs00156373_m1), and VEGF (Hs00173626_m1). The reaction efficiency for each gene was calculated after obtaining standard curves for each PCR reaction by making 2-fold serial dilutions covering the range equivalent to 20 to 0.625 ng RNA (5-0.125 ng for 18S rRNA). Relative quantitation of gene expression was done using the method described by Pfaffl (21). The relative ratio of gene expression was calculated as $[(\text{Etarget})^{\Delta\text{CtTARGET(mean comparator} - \text{mean sample)}}] \div [(\text{Eref})^{\Delta\text{CtREF(mean comparator} - \text{mean sample)}}]$, where Etarget is reaction efficiency of the gene of interest; Eref, reaction efficiency of the reference gene; and ΔCt, the cycle difference between the comparator and the sample. All calculations are based on the mean value of PCR reactions done in triplicate. The comparator for the clinical samples was the median normal kidney; the comparator for cell line work is stated accordingly in the figure legends.

Reverse transcription-PCR. Standard PCR reactions were done using HotStarTaq DNA polymerase (Qiagen, Valencia, CA). In brief, 2× HotStarTaq master mix was combined with 1 μmol/L primers and 5 ng cDNA in a total volume of 20 μL. PCR cycling was done for 38 cycles. PCR products were separated on 1.7% agarose gels stained with ethidium bromide. The following primer sequences were used:

Gene	Forward primer sequence	Reverse primer sequence	Size (bp)
Notch1	CAGGCAATCCG AGGACTATG	CAGGCGTGTTG TTCTCACAG	428
Notch2	CACTGGGTCGA TGATGAAGG	ATCTGGAAGAC ACCTTGGGC	515
Notch3	TCTTGCTGCTG GTCATTCTC	TGCCTCATCCT CTTCAGTTG	485
Notch4	CACTGAGCCAA GGCATAGAC	ATCTCCACCTC ACACCACTG	471
Jagged1	TCGCTGTATCT GTCCACCTG	AGTCACTGGCA CGGTTGTAG	227
Jagged2	GATTGGCGGCT ATTACTGTG	AGGCAGTCGTC AATGTTCTC	600
DLL1	AGAAAGTGTGC AACCCTGGC	GCTCCCTCCGT TCTTACAAG	401
DLL3	GTGAATGCCGA TGCCTAGAG	GGTCCATCTGC ACATGTCAC	256
DLL4	TGACCACTTCG GCCACTATG	AGTTGGAGCCG GTGAAGTTG	620
HES1	TGGATGCGGAG TCTACGATG	TAAGGCCACTT GCCACCTTC	468
HES5	GAAAAACCGAC TGCGGAAGC	GGAAGTGGTAC AGCAGCTTC	314
HES7	TCGAGCTGAGA ATAGGGACG	GAAACCGGACA AGTAGCAGC	274
HEY1	GCCAGCATGA AGCGAGCTC	GGGTCAGAGGC ATCTAGTCC	453
HEY2	AGATGCTTCAG GCAACAGGG	CTGAATCCGCA TGGGCAAAC	408
HEYL	AGAAAGCCGAG GTCTTGCAG	GTAAGCAGGAG AGGAGACAC	389
β-actin	CATCACCATTG GCAATGAGC	CGATCCACACG GAGTACTTG	284

***In vitro* angiogenesis assays.** *In vitro* angiogenesis assays included endothelial cell proliferation, network formation, migration, and scratch wound closure. For the cell proliferation assays, 3×10^4 HUVECs were seeded in triplicate 24 hours posttransfection into 24-well plates precoated with 0.2% gelatin and grown in 0.5 mL culture medium. After 24 hours, medium was removed, cells washed with PBS, trypsinized, and counted using a Beckman Z2 Coulter counter (Fullerton, CA; ref. 22). Thymidine incorporation assay (23) was done by seeding 2×10^3 HUVECs in triplicate, 24 hours posttransfection in 96-well plates. After 24 hours, 1 Ci/mL (1 Ci = 37 kBq) of [*methyl*-^{3}H]thymidine (Amersham Biosciences, Chalfont St. Giles, United Kingdom) was added to each well and incubated for 16 hours. Thymidine incorporation was assessed using a Wallac 1450 microbeta liquid scintillation counter.

For the matrigel network formation assay, each well of a 24-well Falcon tissue culture plate was evenly coated with 250 μL Matrigel (BD Biosciences, Bedford, MA). 4×10^4 HUVECs were seeded 24 hours posttransfection in triplicate per well in MCDB131 + 20% FCS + ECGS. Network formation was assessed after 16 hours by photographing the matrices using a Zeiss Axiovet 135 inverted light microscope and a Nikon CoolPix 4500 digital camera. Quantification of tube formation was done using Adobe Photoshop 7.0.

For the cell migration assays, following transfection and quiescing for 24 hours, 5×10^4 cells were seeded in triplicate in MCBD131 + 1% FCS into the insert well of the BD BioCoat Endothelial Cell Migration Assay plate (BD Biosciences; ref. 24). Migration across the microporous membrane occurred in response to stimuli within the lower chamber (MCDB131 + 5% FCS, MCBD131 + 1% FCS + 10 ng/mL $VEGF_{165}$; R&D Systems, Minneapolis, MN). Following a 22-hour incubation, the cells were labeled with Calcein AM (Molecular Probes, Eugene, OR) and the fluorescent signal from the

Downloaded from cancerres.aacrjournals.org on May 9, 2015. © 2005 American Association for Cancer Research.

undersurface of the membrane measured using a BMG FLUOstar fluorescence plate reader. Images of the insert well were captured using a Zeiss Axiovet 135 inverted light microscope and an Axiocam digital camera.

Scratch wound assay was done as described (25). Twenty-four hours after transfection, 4×10^5 HUVECs were seeded in triplicate into a six-well Falcon tissue culture plate. Cells were fluorescently labeled with 5 μmol/L CMFDA CellTracker dye (Molecular Probes); after which, the monolayer was "scratched" and incubated in MCDB131 + 10% FCS + 50 ng/mL VEGF + 2.5 μg/mL Mitomycin C (Sigma-Aldrich). The wounded area was photographed using a Zeiss Axiovet 135 inverted light microscope and a Nikon CoolPix 4500 digital camera. Quantitation of wound width was done using Adobe Photoshop 7.0.

Cell cycle analysis. Twenty-four hours after transfection, synchronization of cell cycles was achieved by culturing HUVECs for 24 hours in MCDB131 + 2% FCS. Cells were subsequently cultured for 24 hours in either MCDB131 + 20% FCS + ECGS or MCDB131 + 2% FCS, and then fixed in 70% ethanol. Cell cycle analysis was done by fluorescence-activated cell sorting analysis after pretreating cells with RNase (100 μg/mL) and staining nuclear DNA with propidium iodide (50 μg/mL, Sigma-Aldrich; ref. 23).

Apoptosis analysis. 1×10^5 HUVECs were seeded in triplicate in MCDB131 + 20% FCS + ECGS into a 24-well Falcon tissue culture plate. After 24 hours, the cells were serum and growth factor deprived using MCDB131 + 1% FCS. Cell viability was assessed by periodically counting the number of adherent cells using the Beckman Z2 Coulter counter. Apoptosis was assessed using the Apo-ONE Homogenous Caspase 3/7 Assay (Promega Corp., Madison, WI; ref. 26). 2×10^4 HUVECs were seeded in triplicate in 100 μL MCDB131 + 20% FCS + ECGS with 100 μL Apo-ONE reagent in a 96-well white-walled tissue culture plate. After 4 hours, fluorescence was measured at 485/530 nm using a Bio-Tek Flx800 fluorescence plate reader.

***In situ* hybridization.** Radioactive *in situ* hybridization on paraffin-embedded sections was done by the *in situ* hybridization service, Cancer Research UK (London), using a method we described previously (17). The probe used in the *in situ* hybridization for DLL4 was a 741 bp fragment located from position 1,775 to 2,516 bp (17).

Western blotting. Protein extraction and Western blotting were done as previously described (27). Antibodies against the following proteins were used for detection: HIF-1α (1:1,000; BD PharMingen, San Diego, CA), HIF-2α (1:1,000; Abcam, Cambridge, MA), p21 (1:100; Calbiochem, San Diego, CA), p27 (1:500; Cell Signaling), retinoblastoma (1:500; BD PharMingen, Bedford, MA), and β-tubulin (1:10,000; Sigma-Aldrich).

Immunohistochemistry. Immunohistochemistry was done as previously described (28). In brief, paraffin-embedded sections were dewaxed, rehydrated, and incubated with the anti-CD34 monoclonal antibody QBEnd 10 (Novocastra, Newcastle, United Kingdom). Visualization was achieved using the EnVision HRP kit (DAKO Cytomation, Carpinteria, CA).

Statistics. Statistical analysis was done using GraphPad Prism. Statistical tests used included *t* test, one-way ANOVA, Mann-Witney, and Spearman's rank correlation coefficient. Statistical significance was taken at a *P* value of <0.05 and is denoted in the figures with an asterisk.

Results

DLL4 expression in renal cancer. *In situ* hybridization was used to study the expression pattern of DLL4 within the vasculature of normal kidney and clear cell-renal cell carcinoma (CC-RCC). Blood vessels were identified by immunostaining for the pan-endothelial marker CD34, which stained only blood vessels. In comparison with CD34, the expression of DLL4 was up-regulated in the tumor endothelium but not in the normal renal vasculature (Fig. 1*A*).

Using quantitative PCR, the expression of DLL4 in 25 CC-RCCs and 7 non–clear cell tumors [5 papillary renal cell carcinomas, 2 transitional cell carcinomas] was compared with 11 normal kidneys. The expression of DLL4 in CC-RCCs (85.0 ± 99) was almost 9 times higher than in normal kidneys (9.6 ± 8.4, $P < 0.001$) and 20 times higher than in non–clear cell tumors (4.3 ± 6.7, $P < 0.001$; Fig. 1*B*). The relative vascularity of the tissues was assessed by measuring the expression of CD34. The expression of DLL4 was quantified in relation to CD34 (DLL4/CD34 ratio = relative expression of DLL4/relative expression of CD34). Renal tumors showed increased vascularity as revealed by the expression of CD34 compared with normal kidneys; tumor samples, however, also displayed a significantly higher ratio of DLL4 to CD34 than normal kidneys ($P < 0.01$; data not shown). The expression of DLL4 in HUVECs was 40 times higher than in normal kidneys and was similar to the level in tumors (DLL4/CD34 ratio = 38). We have previously shown that microvessel density and the protein level of VEGF are higher in CC-RCCs than in non–clear cell tumors and normal kidneys (28). Using quantitative PCR, we showed that the RNA level of VEGF was also significantly higher in CC-RCCs than in normal tissues and other tumor types ($P < 0.001$; data not shown). Comparison of the expressions of DLL4 and VEGF in CC-RCCs showed that the expression of DLL4 is significantly associated with high levels of VEGF. The Spearman rank correlation coefficient for CC-RCC was 0.75 ($P < 0.0001$; Fig. 1*C*).

Regulation of DLL4 by hypoxia and angiogenic growth factors. Quantitative PCR was used to study DLL4 expression in five endothelial cell lines, including HUVEC, HAEC, HIAEC, HFAEC, and Endo742, cultured at subconfluence in MCDB131 + 20% FCS + ECGS. The expression of DLL4 was highest in HFAEC,

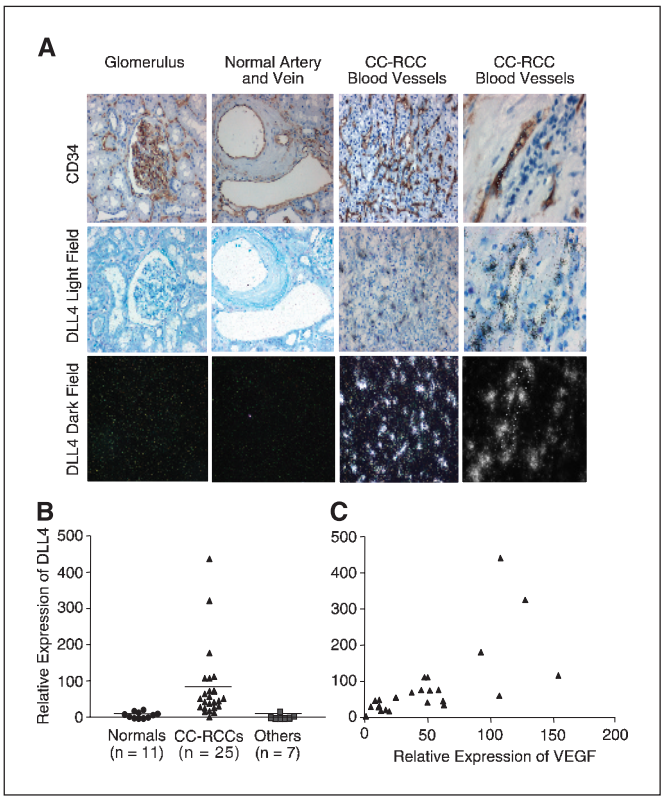

Figure 1. Expression of DLL4 in renal cancer. *A,* the expression pattern of DLL4 was studied using *in situ* hybridization and compared with the endothelial marker CD34, assessed by immunochemistry. DLL4 signal was undetectable in normal renal tissue (magnification, ×200); however, a number of vessels within the vasculature of a CC-RCC showed high levels of expression (magnification, ×500). One of the vessels was marked with a dot line. *B,* quantitative PCR was used to assess the expression of DLL4 in renal tissues (comparator: median normal kidney). DLL4 expression was significantly higher in CC-RCC compared with non–clear cell tumors ($P < 0.001$) and normal renal tissue ($P < 0.001$). *C,* there was a positive correlation between VEGF and DLL4 expression in the CC-RCCs (Spearman rank correlation coefficient = 0.75, $P < 0.0001$, $n = 25$).

Downloaded from cancerres.aacrjournals.org on May 9, 2015. © 2005 American Association for Cancer Research.

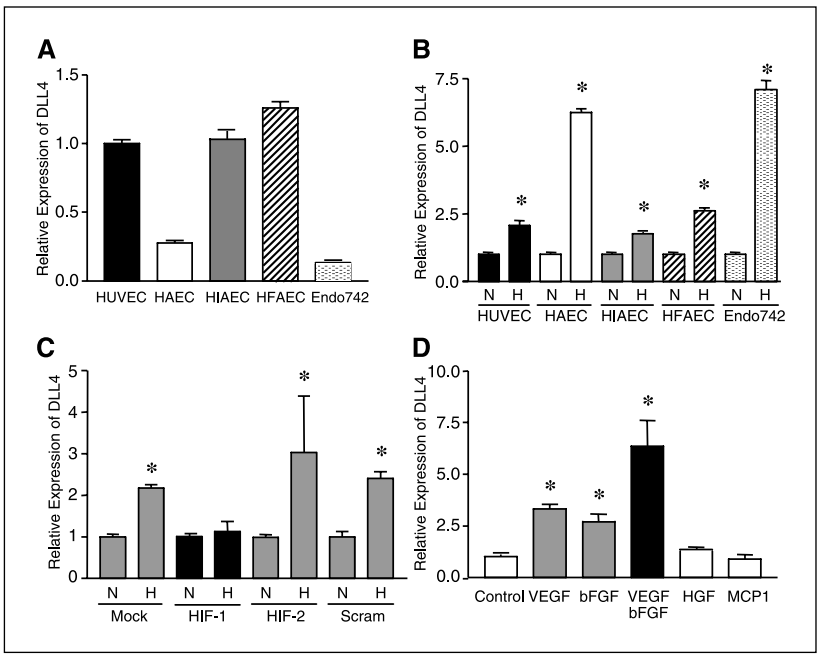

Figure 2. DLL4 is regulated by hypoxia, VEGF, and bFGF. *A,* the relative expression of DLL4 in HUVECs was measured using quantitative PCR (comparator: HUVEC). The basal expression of DLL4 in HUVECs was comparable to expression levels in arterial endothelial cells ($n = 3$). *B,* DLL4 expression was significantly increased in all five cell lines tested following hypoxic incubation ($P < 0.05$, $n = 3$; comparator: normoxia). *C,* siRNA duplexes were used to silence the expression of HIF-1 and HIF-2 in HUVECs. Down-regulation of HIF-1, but not of HIF-2, blocked the hypoxic up-regulation of DLL4 in HUVECs ($n = 4$; comparator: normoxia). *D,* DLL4 expression was significantly up-regulated by VEGF (100 ng/mL) and bFGF (15 ng/mL; $P < 0.05$, $n = 3$); a combination of the two led to a further increase [$P < 0.001$, $n = 3$; comparator: control (MCDB131 + 2% FCS)]. *N,* normoxia; *H,* hypoxia.

with similar expression in HIAEC and HUVEC. DLL4 expression was lowest in HAEC and Endo742 (Fig. 2*A*). DLL4 was up-regulated by hypoxia in all these cell lines. Cells with high basal expression (HUVEC, HIAEC, and HFAEC) showed a 2- to 3-fold induction whereas those with low basal expression showed a 6- to 7-fold increase in DLL4 expression (Fig. 2*B*). HIF-1α and HIF-2α in HUVEC were selectively silenced using siRNA (27). Hypoxic up-regulation of the DLL4 expression was preserved in the mock transfection, scrambled control, and HIF-2α groups, but disappeared in the HIF-1α group, indicating that DLL4 is a HIF-1–regulated gene (Fig. 2*C*).

The regulation of DLL4 expression by various angiogenic growth factors was also assessed. HUVECs were first quiesced for 24 hours in MCBD131 + 2% FCS and then were cultured for 24 hours in MCDB131 + 2% FCS ± growth factor. 100 ng/mL $VEGF_{165}$ and 10 ng/mL basic fibroblast growth factor (bFGF; ref. 29) increased DLL4 expression 2.5- to 3-fold ($P < 0.05$) whereas a combination of the two increased expression 6-fold ($P < 0.001$). However, hepatocyte growth factor (20 ng/mL) and macrophage chemoattractant protein-1 (20 ng/mL) did not influence DLL4 expression (Fig. 2*D*).

The effects of silencing DLL4 using small interfering RNA. Reverse transcription-PCR (RT-PCR) was used to determine which key components of the Notch pathway were expressed by endothelial cells. HUVECs express all four Notch receptors (Notch1-4), four ligands (Jagged1, Jagged2, DLL1, and DLL4), HES1, HEY1, HEY2, and HES7 (weak), but not DLL3, HES5, or HEYL (Fig. 3*A*). Two different siRNA duplexes specific for DLL4 were used to modulate the expression of DLL4 in HUVECs; DLL4 knockdown was evident up to 4 days posttransfection.

Quantitative PCR was then used to further assess the effects of silencing basal DLL4 on key downstream genes including the previously identified bHLH proteins, VEGFR2, and EphrinB2. Down-regulating DLL4 by 80% led to a 60% decrease in HEY1 expression ($P < 0.01$) and a 40% decrease in EphrinB2 expression ($P < 0.05$). There was no significant change in the expression levels of HES1, HEY2, or VEGFR2 following DLL4 RNA interference (RNAi; Fig. 3*B*).

The effect of DLL4 silencing on endothelial cell proliferation. The proliferation of HUVECs transfected with siRNA duplexes specific for DLL4 (Duplex1 and Duplex2) was significantly inhibited compared with mock transfection and scrambled control ($P < 0.001$; Fig. 4*A*). This effect was also shown in Endo742 (data not shown), but not in RT112 (Fig. 4*B*), a transitional cell carcinoma cell line which does not express DLL4. The inhibition of proliferation was further confirmed using a [^{3}H]thymidine uptake assay (data not shown).

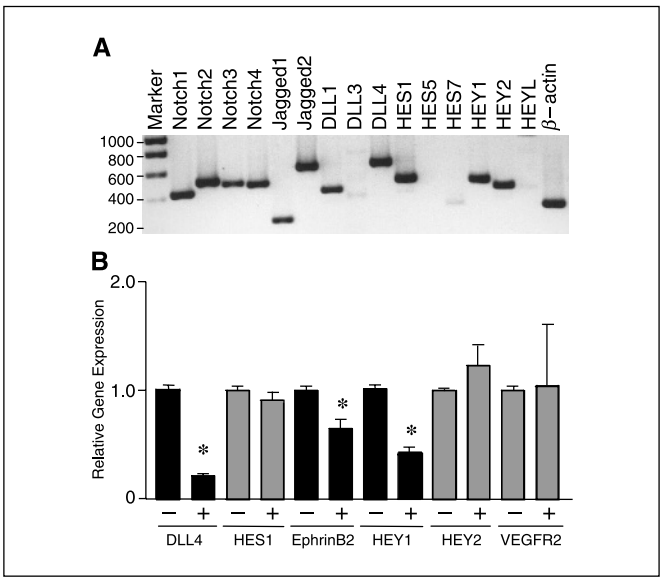

Figure 3. Expression of Notch pathway components in HUVECs and the analysis of the expression of DLL4 and downstream genes following RNAi. *A,* RT-PCR was used to analyze the expression of a variety of Notch components in HUVECs. *B,* quantitative PCR was used to further assess changes in the expression levels of some key downstream genes following transfection of DLL4 Duplex1 (+) into HUVECs. Results of five separate experiments. Eighty-percent knockdown of DLL4 was consistently achieved ($P < 0.001$). This was associated with significant decreases in the expression of EphrinB2 ($P < 0.05$) and HEY1 ($P < 0.01$). Comparator: Scram (−).

Downloaded from cancerres.aacrjournals.org on May 9, 2015. © 2005 American Association for Cancer Research.

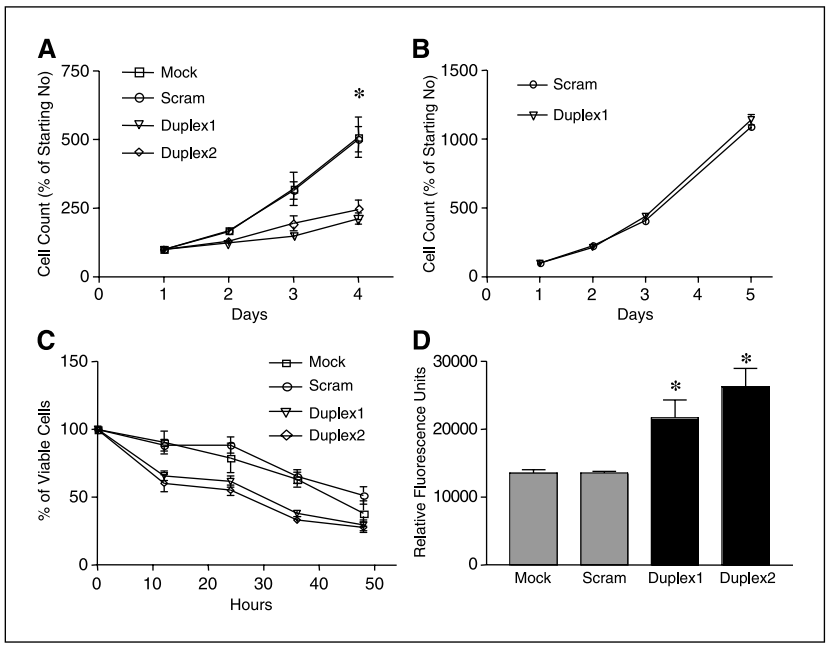

Figure 4. Down-regulation of DLL4 inhibits endothelial cell proliferation and increases apoptosis following serum starvation. *A,* cell count assay showed an inhibition of proliferation in HUVECs following treatment with two siRNA duplexes specific for DLL4 ($P < 0.001$, $n = 9$). *B,* no inhibition of proliferation was shown in the bladder cell line RT112 ($n = 3$). *C,* silencing DLL4 expression in HUVECs significantly decreased cell survival following serum and growth factor deprivation in MCBD131 + 1% FCS ($P < 0.01$, $n = 9$). *D,* the decrease was associated with an increase in caspase-3/-7 activity in HUVECs treated with Duplex1 and Duplex2 ($P < 0.01$, $n = 9$).

DLL4 down-regulation did not induce apoptosis in HUVECs cultured in serum- and growth factor–rich medium (MCDB131 + 20% FCS + ECGS; data not shown), but led to increased apoptosis of the cells following serum and growth factor deprivation. The number of viable cells was significantly ($P < 0.01$) lower following transfection with Duplex1 and 2 when compared with mock and scrambled controls (Fig. 4*C*). Treatment with Duplex1 and 2 was associated with a significant increase in caspase-3/-7 activity (Fig. 4*D*).

Analysis of HUVECs stained with propidium iodide showed that DLL4 knockdown led to cell cycle arrest in G_0-G_1 (Fig. 5*A*). After serum and growth factor stimulation, 28.3% (±9.3 SE) of cells transfected with scrambled control were in S phase compared with 2.54% (±0.8 SE) for Duplex1 ($P < 0.01$) and 10.4% (±3.4 SE) for Duplex2 ($P < 0.05$; Fig. 5*B*). Down-regulation of DLL4 increased levels of p21 and decreased levels of the phosphorylated retinoblastoma. No change was noted for the p27 protein (Fig. 5*C*).

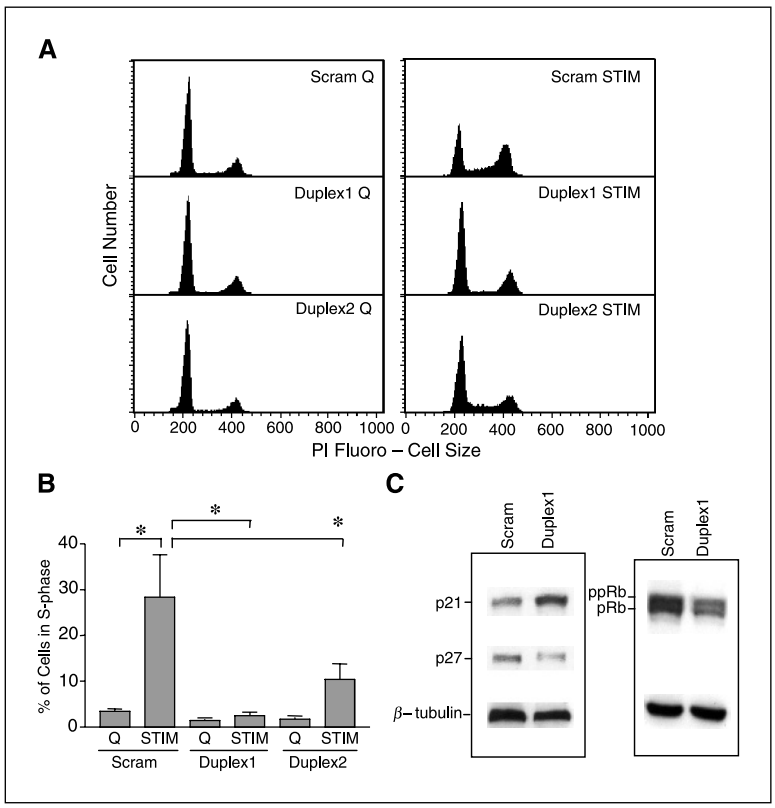

Figure 5. DLL4 knockdown induces cell cycle arrest by increasing p21 expression and inhibiting retinoblastoma phosphorylation. *A,* propidium iodide–based cell cycle analysis was done following siRNA transfection. Synchronization of cell cycles was achieved by culturing in MCDB131 + 2% FCS for 24 hours. Subsequently, cells were cultured for 24 hours in either MCDB131 + 2% FCS only (Scram Q, Duplex1 Q, and Duplex2 Q) or MCDB131 + 20% FCS + ECGS (Scram STIM, Duplex1 STIM, and Duplex2 STIM). HUVECs treated with siRNA specific for DLL4 seem to arrest in G_0-G_1 and did not progress through the cell cycle following growth factor and serum stimulation compared with scrambled control. *B,* S-phase analysis showed that 28.36% (±9.3 SE) of Scram STIM cells were in S phase compared with 2.54% (±0.8 SE) for Duplex1 ($P < 0.01$) and 10.41% (±3.4 SE) for Duplex2 ($P < 0.01$; $n = 3$). *C,* Western blot analysis showed that down-regulation of DLL4 in HUVECs leads to increased expression of p21 and decreased phosphorylation of retinoblastoma ($n = 3$).

Downloaded from cancerres.aacrjournals.org on May 9, 2015. © 2005 American Association for Cancer Research.

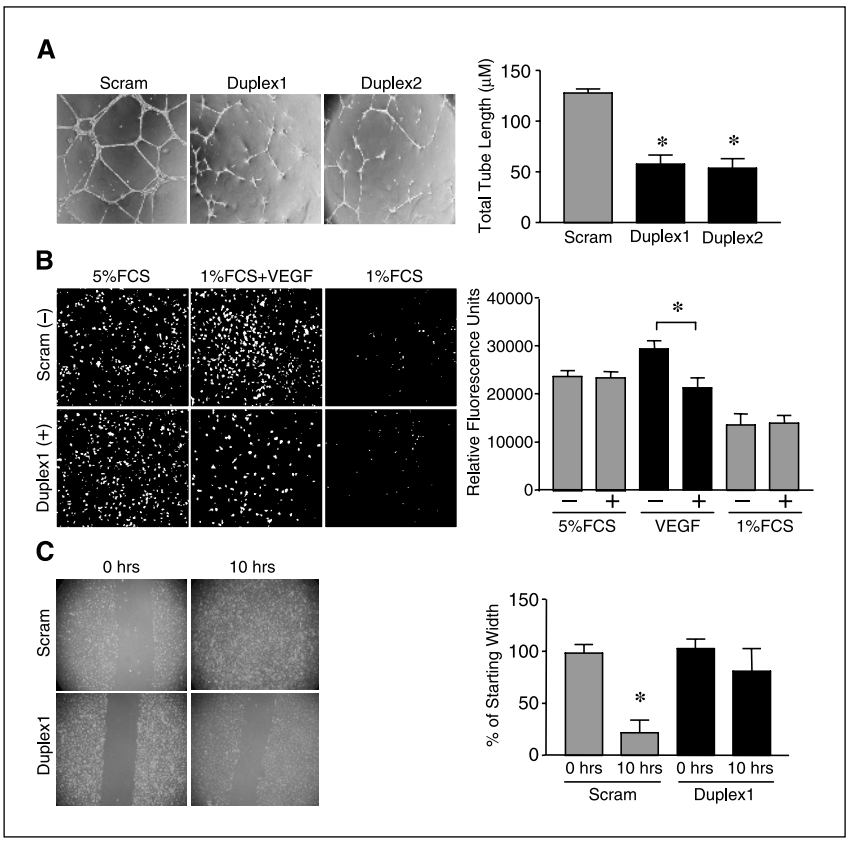

Figure 6. Down-regulation of basal DLL4 expression inhibits endothelial cell network formation and migration. *A,* endothelial cell network formation was assessed using a Matrigel assay. Representative areas were photographed at ×15 magnification and quantified using Adobe Photoshop. Down-regulation of DLL4 in HUVECs led to a significant decrease in total tube length compared with scrambled control ($P < 0.001$, $n = 9$). *B,* endothelial cell migration was assessed using a BD BioCoat Migration Plate. Down-regulation of DLL4 inhibits VEGF (10 ng/mL)–stimulated migration in HUVECs ($P < 0.01$, $n = 9$). No modulation of serum-stimulated migration was noted. *C,* HUVEC migration was further assessed using a scratch wound assay. Wound closure in response to VEGF stimulation (50 ng/mL) was significantly reduced following DLL4 knockdown ($P < 0.001$, $n = 9$).

The effects of modulation of DLL4 expression on endothelial cell network formation and migration. A reduction in the basal levels of DLL4 led to decreased network formation in matrigel (Fig. 6*A*). Network formation, as judged by total tube length, was significantly lower ($P < 0.001$) following treatment with Duplex1 and Duplex2 compared with scrambled control.

BD BioCoat Endothelial Cell Migration plates were used to study the effects of silencing DLL4 on HUVEC migration. HUVECs in which DLL4 was silenced were less responsive to VEGF-induced migration compared with scrambled control ($P < 0.01$). There was no difference when FCS alone was used to stimulate migration (Fig. 6*B*). Endothelial cell migration was further analyzed using the scratch wound assay. Down-regulation of DLL4 using siRNA significantly ($P < 0.001$) inhibited VEGF-stimulated wound closure when compared with scrambled control (Fig. 6*C*).

Discussion

In this study, we described that the expression of DLL4, as assessed by quantitative PCR, was strikingly up-regulated in CC-RCCs, consistent with our previous *in situ* hybridization work on five renal cancer/normal pairs (17). This is the first quantitative evaluation of the frequency and extent of DLL4 up-regulation in cancer. CC-RCC, the most common type of malignant renal tumor, accounting for 70% to 80% of cases (30), occurs in both a hereditary and sporadic form, both of which are associated with mutations in the von Hippel-Lindau (*VHL*) gene (31, 32).

Although DLL4 was undetectable in adult endothelium *in vivo*, we found, as have others, that several primary endothelial cells do express it *in vitro* (29, 33–35). The ratio of DLL4 to CD34 in HUVECs is similar to that found in the highest expressing CC-RCCs. We therefore chose HUVEC as a model to investigate the biological function of DLL4 in tumor angiogenesis. We confirmed that DLL4 is a hypoxia-regulated gene and proved that the hypoxic regulation is dependent on HIF-1 rather than HIF-2.

We showed that the expression of DLL4 in HUVECs is up-regulated by VEGF and bFGF, and their combination leads to a synergistic further increase in expression. Indeed, the combination of VEGF and bFGF can induce DLL4, Notch1, and Notch4 in HUVECs (29). The regulation of DLL4 by VEGF *in vitro* and the significant correlation between DLL4 and VEGF expression in CC-RCCs imply that VEGF may act upstream of DLL4 in the tumors. It is noted that VEGF can act upstream of DLL4 and Notch4 in the determination of arterial endothelial cell fate in zebra fish (36). bFGF is also produced by renal cancers (37) through a non-HIF pathway. Thus, the combination of VEGF and bFGF may contribute to the high expression of DLL4 within the tumor vasculature.

Using conventional RT-PCR, we showed that HUVECs express all four Notch receptors, four ligands (Jagged1, Jagged2, DLL1, and DLL4), and four bHLH transcription factors [HES1, HEY1, HEY2, and HES7 (weak)], but not DLL3, HES5, and HEYL. Indeed, other groups (29, 35) have shown that HUVECs express Notch1, Notch4, and DLL4, whereas there is also a report indicating that HUVECs express Notch1, 2, 3, and 4 and Jagged1, but not DLL4 (33). The discrepancy for the expression of Notch receptors and ligands in HUVECs may reflect cell heterogeneity or variations between cell batches.

Several groups have attempted to unravel the role of the Notch pathway in endothelial cell biology via the overexpression of Notch signaling components (Jagged1, HES1, and HEY1) or the active Notch intracellular domain of Notch1 and Notch4 (29, 33, 35, 38, 39). Clearly, there are problems of induced high expression, particularly

Downloaded from cancerres.aacrjournals.org on May 9, 2015. © 2005 American Association for Cancer Research.

relating to physiologic significance. Therefore, we assessed the biological function of DLL4 by using RNAi to reduce its endogenous expression. Down-regulating DLL4 by 80% led to significant decreases in the expression levels of EphrinB2 and HEY1, indicating a basal role of the DLL4 expression in the regulation of these pathways. HUVECs express several Notch ligands (Jagged1, Jagged2, DLL1, and DLL4); however, regulation of DLL4 alone had substantial effects, suggesting that it is one of the main ligands regulating basal Notch function in endothelial cells. Surprisingly, we have shown that silencing DLL4 in endothelial cells leads to a significant inhibition of proliferation, a result previously found for overexpression studies. The inhibition is due to the arrest of cell cycle in G_0-G_1, an effect mediated by an increase in levels of p21 and a decrease in the phosphorylation of retinoblastoma. The induction of p21 and resultant decreased phosphorylation of retinoblastoma have previously been shown to induce G_0-G_1 cell cycle arrest in HUVECs (40–42). However, overexpression of Notch4 or knockout of Notch1 and Notch4 produces similar phenotypes (43, 44). Taken together, this suggests that an optimal range of the Notch signaling is important in the proliferation of endothelial cells.

The effects on apoptosis were reciprocal. We showed that silencing DLL4 induces apoptosis in HUVECs, only following deprivation of serum and growth factors. Overexpression of Notch1, Notch4, or HES1 protects primary endothelial cells against serum starvation–induced apoptosis and inhibits lipopolysaccharide-induced apoptosis (29).

We showed that down-regulation of DLL4 reduces the network formation of HUVECs on matrigel. Up-regulation of Notch1 or HES1 results in stabilization of network formation, whereas inhibition of Notch signaling with a dominant-negative CSL partially inhibits VEGF-driven network formation in HIAECs (29). However, both overexpression and reduction of HEY1 with antisense oligonucleotides blocked endothelial cell network formation *in vitro* (45). Using the trans-well migration assay and the scratch wound technique, we showed that DLL4 knockdown leads to significant inhibition of VEGF-driven endothelial cell migration. Activated Notch4 inhibits HMEC-1 migration across collagen in response to VEGF and FGF (46), but not through fibrinogen, by increasing the activity and affinity of surface-bound β1-integrin (47), whereas overexpression of HES1 in endothelial cells decreases migration in response to VEGF or bFGF (45). Thus, again the surprising result is that the effects of down-regulation of DLL4 are similar to the effects of up-regulation of Notch signaling.

In summary, we have quantitatively shown for the first time that the expression of DLL4 is up-regulated in CC-RCCs and that the reduction of basal DLL4 expression has profound effects on multiple endothelial functions important in tumor angiogenesis. Down-regulation of DLL4 produces many phenotypic features displayed by up-regulation of the Notch pathway. Therefore, we propose that an optimal window of the DLL4 expression is essential for tumor angiogenesis. The selective modulation of the DLL4 expression within human tumors may represent a potential novel antiangiogenic therapy.

Acknowledgments

Received 4/8/2005; revised 5/27/2005; accepted 6/17/2005.

Grant support: Cancer Research UK (J-L. Li, D. Generali, and A.L. Harris), the 6th Framework Programme of the European Union (Angiotargeting), and the Royal College of Surgeons of England and the British Urological Foundation (N.S. Patel).

The costs of publication of this article were defrayed in part by the payment of page charges. This article must therefore be hereby marked *advertisement* in accordance with 18 U.S.C. Section 1734 solely to indicate this fact.

We thank Cassin Kimmel, Richard Poulsom, Mike Dobby, Sarah Pratap, and Roy Bicknell for their help and advice.

References

1. Folkman J. Tumor angiogenesis: therapeutic implications. N Engl J Med 1971;285:1182–6.
2. Harris AL. Hypoxia—a key regulatory factor in tumour growth. Nat Rev Cancer 2002;2:38–47.
3. Artavanis-Tsakonas S, Matsuno K, Fortini ME. Notch signaling. Science 1995;268:225–32.
4. Weinmaster G. The ins and outs of notch signaling. Mol Cell Neurosci 1997;9:91–102.
5. Radtke F, Raj K. The role of Notch in tumorigenesis: oncogene or tumour suppressor? Nat Rev Cancer 2003;3:756–67.
6. Mumm JS, Kopan R. Notch signaling: from the outside in. Dev Biol 2000;228:151–65.
7. Weinmaster G. Notch signaling: direct or what? Curr Opin Genet Dev 1998;8:436–42.
8. Nakagawa O, McFadden DG, Nakagawa M, et al. Members of the HRT family of basic helix-loop-helix proteins act as transcriptional repressors downstream of Notch signaling. Proc Natl Acad Sci U S A 2000;97:13655–60.
9. Davis RL, Turner DL. Vertebrate hairy and Enhancer of split related proteins: transcriptional repressors regulating cellular differentiation and embryonic patterning. Oncogene 2001;20:8342–57.
10. Iso T, Kedes L, Hamamori Y. HES and HERP families: multiple effectors of the Notch signaling pathway. J Cell Physiol 2003;194:237–55.
11. Iso T, Hamamori Y, Kedes L. Notch signaling in vascular development. Arterioscler Thromb Vasc Biol 2003;23:543–53.
12. Duarte A, Hirashima M, Benedito R, et al. Dosage-sensitive requirement for mouse Dll4 in artery development. Genes Dev 2004;18:2474–8.
13. Krebs LT, Shutter JR, Tanigaki K, Honjo T, Stark KL, Gridley T. Haploinsufficient lethality and formation of arteriovenous malformations in Notch pathway mutants. Genes Dev 2004;18:2469–73.
14. Gale NW, Dominguez MG, Noguera I, et al. Haploinsufficiency of delta-like 4 ligand results in embryonic lethality due to major defects in arterial and vascular development. Proc Natl Acad Sci U S A 2004;101:15949–54.
15. Ferrara N, Carver-Moore K, Chen H, et al. Heterozygous embryonic lethality induced by targeted inactivation of the VEGF gene. Nature 1996;380:439–42.
16. Carmeliet P, Ferreira V, Breier G, et al. Abnormal blood vessel development and lethality in embryos lacking a single VEGF allele. Nature 1996;380:435–9.
17. Mailhos C, Modlich U, Lewis J, Harris A, Bicknell R, Ish-Horowicz D. Delta4, an endothelial specific notch ligand expressed at sites of physiological and tumor angiogenesis. Differentiation 2001;69:135–44.
18. Claxton S, Fruttiger M. Periodic delta-like 4 expression in developing retinal arteries. Gene Expr Patterns 2004;5:123–7.
19. O'Hare MJ, Bond J, Clarke C, et al. Conditional immortalization of freshly isolated human mammary fibroblasts and endothelial cells. Proc Natl Acad Sci U S A 2001;98:646–51.
20. Brown D, Jarvis R, Pallotta V, Byrom M, Ford L. RNA interference in mammalian cell culture: design, executin and analysis of the siRNA effect. Ambion TechNotes 2002;9:3–5.
21. Pfaffl MW. A new mathematical model for relative quantification in real-time RT-PCR. Nucleic Acids Res 2001;29:e45.
22. Robertson N, Potter C, Harris AL. Role of carbonic anhydrase IX in human tumor cell growth, survival, and invasion. Cancer Res 2004;64:6160–5.
23. Ho PY, Liang YC, Ho YS, Chen CT, Lee WS. Inhibition of human vascular endothelial cells proliferation by terbinafine. Int J Cancer 2004;111:51–9.
24. Suchting S, Heal P, Tahtis K, Stewart LM, Bicknell R. Soluble Robo4 receptor inhibits *in vivo* angiogenesis and endothelial cell migration. FASEB J 2005;19:121–3.
25. Erzurum VZ, Bian JF, Husak VA, et al. R136K fibroblast growth factor-1 mutant induces heparin-independent migration of endothelial cells through fibrin glue. J Vasc Surg 2003;37:1075–81.
26. Goodwin BL, Solomonson LP, Eichler DC. Argininosuccinate synthase expression is required to maintain nitric oxide production and cell viability in aortic endothelial cells. J Biol Chem 2004;279:18353–60.
27. Sowter HM, Raval RR, Moore JW, Ratcliffe PJ, Harris AL. Predominant role of hypoxia-inducible transcription factor (Hif)-1α versus Hif-2α in regulation of the transcriptional response to hypoxia. Cancer Res 2003;63:6130–4.
28. Turner KJ, Moore JW, Jones A, et al. Expression of hypoxia-inducible factors in human renal cancer: relationship to angiogenesis and to the von Hippel-Lindau gene mutation. Cancer Res 2002;62:2957–61.
29. Liu ZJ, Shirakawa T, Li Y, et al. Regulation of Notch1 and Dll4 by vascular endothelial growth factor in arterial endothelial cells: implications for modulating arteriogenesis and angiogenesis. Mol Cell Biol 2003;23:14–25.
30. Reuter VE, Presti JC, Jr. Contemporary approach to the classification of renal epithelial tumors. Semin Oncol 2000;27:124–37.
31. Herman JG, Latif F, Weng Y, et al. Silencing of the VHL tumor-suppressor gene by DNA methylation in renal carcinoma. Proc Natl Acad Sci U S A 1994;91:9700–4.
32. Gnarra JR, Tory K, Weng Y, et al. Mutations of the

Downloaded from cancerres.aacrjournals.org on May 9, 2015. © 2005 American Association for Cancer Research.

VHL tumour suppressor gene in renal carcinoma. Nat Genet 1994;7:85–90.
33. Noseda M, Chang L, McLean G, et al. Notch activation induces endothelial cell cycle arrest and participates in contact inhibition: role of p21Cip1 repression. Mol Cell Biol 2004;24:8813–22.
34. Nakatsu MN, Sainson RC, Aoto JN, et al. Angiogenic sprouting and capillary lumen formation modeled by human umbilical vein endothelial cells (HUVEC) in fibrin gels: the role of fibroblasts and Angiopoietin-1. Microvasc Res 2003;66:102–12.
35. Taylor KL, Henderson AM, Hughes CC. Notch activation during endothelial cell network formation *in vitro* targets the basic HLH transcription factor HESR-1 and down-regulates VEGFR-2/KDR expression. Microvasc Res 2002;64:372–83.
36. Lawson ND, Vogel AM, Weinstein BM. sonic hedgehog and vascular endothelial growth factor act upstream of the Notch pathway during arterial endothelial differentiation. Dev Cell 2002;3:127–36.
37. Nanus DM, Schmitz-Drager BJ, Motzer RJ, et al. Expression of basic fibroblast growth factor in primary human renal tumors: correlation with poor survival. J Natl Cancer Inst 1993;85:1597–9.
38. MacKenzie F, Duriez P, Wong F, Noseda M, Karsan A. Notch4 inhibits endothelial apoptosis via RBP-Jκ-dependent and -independent pathways. J Biol Chem 2004;279:11657–63.
39. Shawber CJ, Das I, Francisco E, Kitajewski J. Notch signaling in primary endothelial cells. Ann N Y Acad Sci 2003;995:162–70.
40. Freedman DA, Folkman J. Maintenance of G_1 checkpoint controls in telomerase-immortalized endothelial cells. Cell Cycle 2004;3:811–6.
41. Bruhl T, Heeschen C, Aicher A, et al. p21Cip1 levels differentially regulate turnover of mature endothelial cells, endothelial progenitor cells, and *in vivo* neovascularization. Circ Res 2004;94:686–92.
42. Yeh JR, Mohan R, Crews CM. The antiangiogenic agent TNP-470 requires p53 and p21CIP/WAF for endothelial cell growth arrest. Proc Natl Acad Sci U S A 2000;97:12782–7.
43. Krebs LT, Xue Y, Norton CR, et al. Notch signaling is essential for vascular morphogenesis in mice. Genes Dev 2000;14:1343–52.
44. Uyttendaele H, Ho J, Rossant J, Kitajewski J. Vascular patterning defects associated with expression of activated Notch4 in embryonic endothelium. Proc Natl Acad Sci U S A 2001;98:5643–8.
45. Henderson AM, Wang SJ, Taylor AC, Aitkenhead M, Hughes CC. The basic helix-loop-helix transcription factor HESR1 regulates endothelial cell tube formation. J Biol Chem 2001;276:6169–76.
46. MacKenzie F, Duriez P, Larrivee B, et al. Notch4-induced inhibition of endothelial sprouting requires the ankyrin repeats and involves signaling through RBP-Jκ. Blood 2004;104:1760–8.
47. Leong KGl, Hu X, Li L, et al. Activated Notch4 inhibits angiogenesis: role of β1-integrin activation. Mol Cell Biol 2002;22:2830–41.

Downloaded from cancerres.aacrjournals.org on May 9, 2015. © 2005 American Association for Cancer Research.

Cancer Research
The Journal of Cancer Research (1916–1930) | The American Journal of Cancer (1931–1940)

Up-regulation of Delta-like 4 Ligand in Human Tumor Vasculature and the Role of Basal Expression in Endothelial Cell Function

Nilay S. Patel, Ji-Liang Li, Daniele Generali, et al.

Cancer Res 2005;65:8690-8697.

Updated version	Access the most recent version of this article at: http://cancerres.aacrjournals.org/content/65/19/8690

Cited Articles	This article cites by 45 articles, 24 of which you can access for free at: http://cancerres.aacrjournals.org/content/65/19/8690.full.html#ref-list-1
Citing articles	This article has been cited by 59 HighWire-hosted articles. Access the articles at: http://cancerres.aacrjournals.org/content/65/19/8690.full.html#related-urls

E-mail alerts	Sign up to receive free email-alerts related to this article or journal.
Reprints and Subscriptions	To order reprints of this article or to subscribe to the journal, contact the AACR Publications Department at pubs@aacr.org.
Permissions	To request permission to re-use all or part of this article, contact the AACR Publications Department at permissions@aacr.org.

Downloaded from cancerres.aacrjournals.org on May 9, 2015. © 2005 American Association for Cancer Research.